Computational study of CO2 injection at Johan Sverdrup for enhanced oil recovery and storage

Hansen, Ole Christopher; Moldestad, Britt Margrethe Emilie

Department of Process, Energy and Environmental Technology - University of South-Eastern Norway

Hansen, O. C., & Moldestad, B. M. (2020). *Computational study of CO2 injection at Johan Sverdrup for enhanced oil recovery and storage*. In Proceedings of The 61st SIMS Conference on Simulation and Modelling SIMS 2020 - Linköping Electronic Conference Proceedings, pp. 311-317, 176(44).
https://doi.org/10.3384/ecp20176311

Publisher's version: DOI: 10.3384/ecp20176311

Computational study of CO_2 injection at Johan Sverdrup for enhanced oil recovery and storage

Ole Christopher Hansen[1] Britt M. E. Moldestad[1]

[1]Department of Process, Energy and Environmental Technology, University of South-Eastern Norway, Norway,
Olechr95@gmail.com Britt.Moldestad@usn.no

Abstract

Injection of supercritical carbon dioxide (CO_2) for enhanced oil recovery (EOR), plays a vital role to minimize the impact of CO_2 emissions. CO_2-EOR refers to the oil recovery technique where supercritical CO_2 is injected in the reservoir to stimulate oil production from depleted oil fields. CO_2-EOR can be used in combination with CO_2 storage to mitigate the emissions levels to the atmosphere. The objective of this paper is to perform a computational study of CO_2-EOR and storage at the Johan Sverdrup field. The study includes simulations of oil production using the commercial software Rocx in combination with OLGA. Production with inflow control devices (ICD) and autonomous inflow control valves (AICV) shows that AICVs have an oil-to-water ratio of 0.92 compared to 0.39 for ICDs. CO_2-EOR in combination with well completion with AICVs, shows improved oil recovery, low water production, and low CO_2 reproduction. The simulations and calculations performed in this paper indicate that the Johan Sverdrup field is highly capable for CO_2-EOR and storage.

Keywords: Increased oil recovery, Johan Sverdrup field, CO_2 EOR, Inflow control devices, OLGA/Rocx simulation

1 Introduction

The oil industry uses several different technologies to increase the oil recovery from new and existing reservoirs. Enhanced Oil Recovery (EOR) can be used in new, existing, and also closed wells to increase the oil production. A possible method for EOR is injection of CO_2 as a supercritical fluid. Supercritical CO_2 has a significantly higher density than CO_2 gas, whereas the viscosity is about the same for the two phases. The positive side effect of injecting CO_2 in reservoirs is the storage possibilities.

Figure 1 shows the expected remaining resources in some of the most significant fields on the Norwegian continental shelf (NCS). According to the Resource report published by the Norwegian Petroleum Directorate in 2019, the number of recoverable resources as of 31st December 2018, was estimated to be 15.6 billion standard cubic meters (Sm^3) of oil equivalent (o.e.), including all the resources previously produced (Norwegian Petroleum Directorate, 2019). The Johan Sverdrup field started up during the autumn 2019 and is considered as the most prominent field development for the past 20 years.

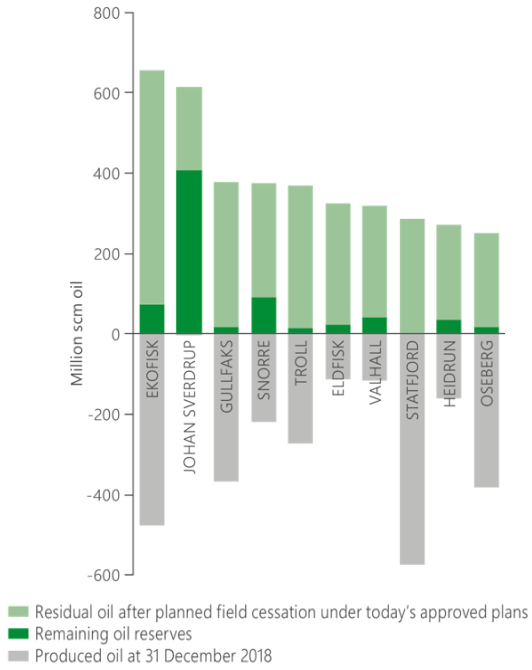

Figure 1. Distribution of oil resources and oil reserves in the 10 largest oil fields on the Norwegian shelf.

The improvements developed concerning horizontal wells in the last decades have made it possible to use long and multilateral wells. Long horizontal and multilateral wells are used to obtain maximum reservoir contact, which results in better production efficiency. Horizontal wells have a frictional pressure drop from the toe to the heel. The heel is located where the well bends from vertical to horizontal, and the toe is the endpoint of the horizontal well. As can be seen in Figure 2, the pressure difference between the reservoir and the well is significantly higher in the heel (ΔP_h) compared to the toe (ΔP_t). This is called the heel-to-toe effect. The pressure difference between reservoir and well is called drawdown, and indicates the driving force for production.

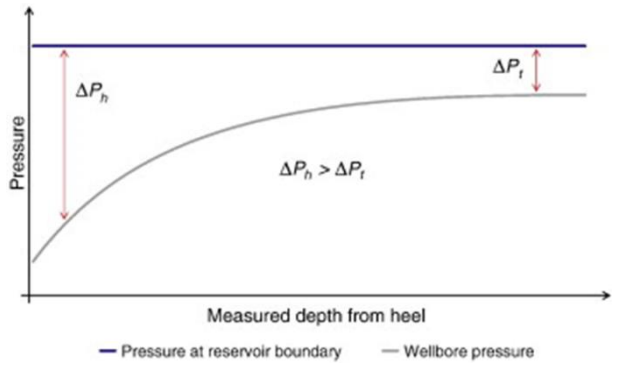

Figure 2. Frictional pressure drop and pressure difference (Birchenko *et al*, 2010)

The motivation for combining CO_2-EOR and storage could open possibilities for long term storage capacity in the future. Increased yield by CO_2-EOR and storage could appear as appealing to customers from an economic standpoint. Storing CO_2 would help towards Norway's goals of becoming a low carbon society by 2050.

2 Inflow control

This section includes the description of two different types of inflow control devices.

2.1 Inflow control devices

Different types of inflow control devices are installed as a part of the well completion to help optimizing the production by adjusting the flow rate along the wellbore. The purpose of these devices is to delay the breakthrough of either gas or water. Delaying the breakthrough is typically done by reducing the annular velocity across each section, such as the heel of a horizontal well. Multiple ICDs are installed with different diameters in each zone in the well. The diameter is smallest near the heel since the drawdown in this area is significantly higher than in the toe section. By installing ICDs with small diameter in the heel section, the flow is reduced and becomes equal to the flow in the toe section. Thus, an even inflow is achieved from all parts of the well, and early breakthrough of water or gas in the heel is avoided. Figure 3 shows how the implementation of ICDs will even out the breakthrough of gas and water, thus increasing production from each well.

The principle of the nozzle ICD is based on the following equations (Aakre, 2017):

$$\Delta P = \frac{\rho v^2}{2C^2} = \frac{\rho \dot{Q}^2}{2A_{Valve}^2 C^2} = \frac{8\rho \dot{Q}^2}{\pi^2 D_{Valve}^4 C^2} \quad (1)$$

$$C = \frac{C_D}{\sqrt{(1-\beta^4)}} = \frac{1}{\sqrt{K}} \quad (2)$$

$$\beta = \frac{D_2}{D_1} \quad (3)$$

ΔP is the pressure drop through the nozzle ICD, ρ is the average fluid density, *v* is fluid velocity through the nozzle, $\dot{\mathbf{Q}}$ is the fluid flow rate through the nozzle, A is the cross-sectional area of the nozzle, C is the flow coefficient, C_D is the discharge rate coefficient, K is the pressure drop coefficient, and D is the diameter of the nozzle. These equations show that the nozzle ICD is independent of the fluid viscosity.

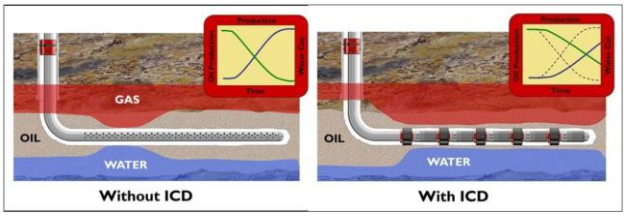

Figure 3. Illustration of water and gas breakthrough without and with ICDs (Halliburton, 2010).

2.2 Autonomous inflow control valves

The autonomous inflow control valve (AICV) can distinguish between fluids based on fluid viscosity and density. The principal operating feature of the AICV is to open for high viscosity fluids and close for low viscosity fluids. This mechanism is controlled by a minor pilot flow that flows parallel to the main flow, and this is shown in Figure 4. The mechanism is described in detail in (Aakre, 2017; Aakre *et al*, 2013; Kais *et al*, 2016; Aakre *et al*, 2018).

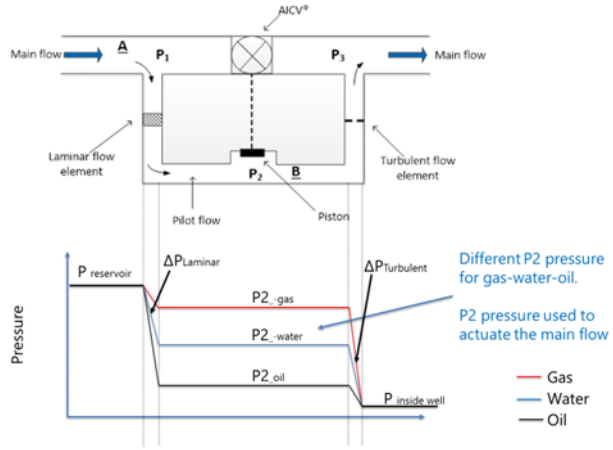

Figure 4. The principle of the AICV (Aakre, 2017).

When the difference in pressure (P_1-P_2) is high, as in the case of oil, the valve stays in the open position. If the pressure difference is low, as in the case of water or gas, the valve will return to the closed position. A closed valve allows for zoning out different sections along the wellbore, thus increasing the recovery of the desired fluid. During production, the AICV is designed to have approximately 99% of the flow rate in the main flow, and when the valve is closed, the minor pilot flow represents the total flow rate through the valve (Aakre, 2017).

The pressure difference can be expressed based on the laminar and turbulent flow elements:

$$\Delta P_{laminar} = f \cdot \frac{L\rho v^2}{2D} = \frac{64}{Re} \cdot \frac{L\rho v^2}{2D} = \frac{32\mu v L}{D^2} \quad (4)$$

where f is the laminar friction factor ($64/Re$), ρ is the fluid density, v is the fluid velocity, μ is the fluid viscosity, D is the diameter of the laminar flow element, and L is the length of the laminar flow element.

$$\Delta P_{turbulent} = k \cdot \frac{\rho v^2}{2} \quad (5)$$

where k is a geometric constant.

3 Material and methods

3.1 Simulation tools

To predict the production of oil and water from a reservoir, simulations have been done in OLGA-Rocx. The OLGA-Rocx module is a dynamic reservoir model designed to model flow rates and pressures near the wellbore. OLGA simulates flow rates and pressures based on the reservoir model defined in Rocx. The simulations are performed over a specified period, and changes are registered over time.

In this study, the conditions from the Johan Sverdrup field in the North Sea were used as a basis for the simulations. As shown in Figure 5, the Johan Sverdrup field is located approximately 150 km west of Stavanger, Norway. Most of the data collected for these simulations are made public by Equinor. However, some values had to be approximated, such as the ratio between horizontal and vertical permeability and the relative permeability.

Figure 5. Geographical location of the Johan Sverdrup field (Equinor, ASA, 2020)

3.1.1 Rocx

The geometry of the reservoir was modeled in Rocx, and is presented in Figure 6. The reservoir is a homogenous sandstone reservoir. The geometry for the simulated reservoir is 1312.5 m in length, 100 m in width and, 40 m in height. 21 grid blocks are defined in the x-direction, 23 grid blocks in the y-direction, and 10 in the z-direction. The well is located 20 m from the bottom, which is indicated by the black circle. The simulated reservoir represents the production area for one well in a large reservoir.

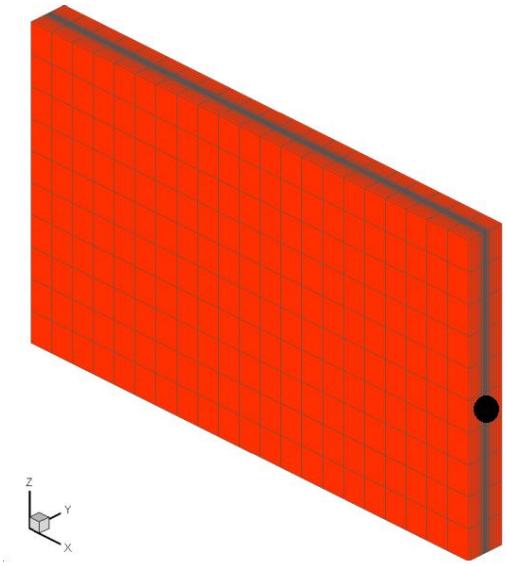

Figure 6. Grid resolution in a reservoir section designed in Rocx. Black dot is the well.

Since the reservoir is homogenous, the porosity and permeability are constant at 0.28 and 5000 mD respectively in the entire reservoir. In these simulations, a ratio between vertical and horizontal permeability of 0.1 is used. The temperature is maintained constant at 83 °C, the water drive pressure is constant at 195 bar, and the wellbore pressure is set to 192 bar in the heel section. The reservoir and fluid properties are presented in Table 1.

Table 1. Reservoir and fluid properties.

Properties	
Oil viscosity	3 cP
Oil density	810 kg/m^3
Reservoir pressure	195 bar
Reservoir temperature	83 °C
Oil specific gravity	0.81
Wellbore pressure (heel)	192 bar
Permeability (x-y-z direction)	5000-5000-500 mD
Porosity	0.28

3.1.2 OLGA

The OLGA simulator is governed by conservation of mass equations for gas, liquid and liquid droplets, conservation of momentum equations for the liquid phase and the liquid droplets at the walls, and conservation of energy mixture equation with phases having the same temperature (Schlumberger Software, 2020).

The OLGA module uses the model developed in Rocx by importing data through the near-well source. To achieve an accurate representation of a wellbore,

with valves, packers, annulus, and production pipe, OLGA requires a "Flowpath" and "Pipeline" (Sund *et al*, 2017) as shown in Figure 7. For an accurate representation of the wellbore, two separate production pipes need to be defined to account for the annulus and production pipe. "Flowpath" is defined as the production pipe, and "Pipeline" is defined as the annulus. The entire well is divided into 42 equal sections. As shown in the figure, the connection to Rocx occurs through the sources. These sources indicate inflow from the reservoir to the annulus. The inflow control (ICD or AICV), together with the leaks, indicate the flow from the annulus into the pipe. The packers are simulated as closed valves, and their purpose is to isolate different production zones in the well. The packers divide the production pipe into 21 zones.

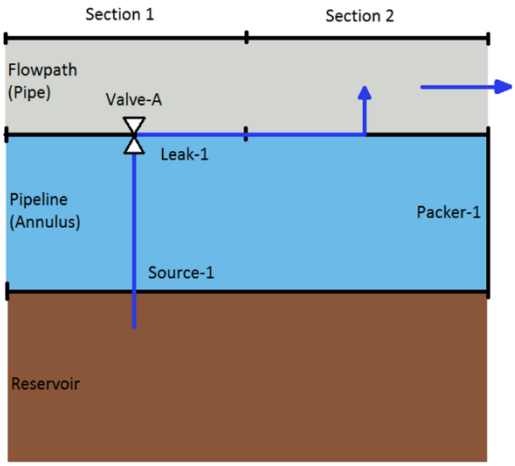

Figure 7. Excerpt of near-well simulation in OLGA.

3.1.3 Simulation set-up for ICD and AICV

Two cases, Case 1 and Case 2, were modelled and simulated. The ICD case (Case 1) was modeled with fully open valves, and in the AICV case (Case 2) the valves were modelled to be adjusted between open and closed based on the nearby fluid properties. In Figure 8, the valve is called VALVE-2 and is either an ICD or an AICV.

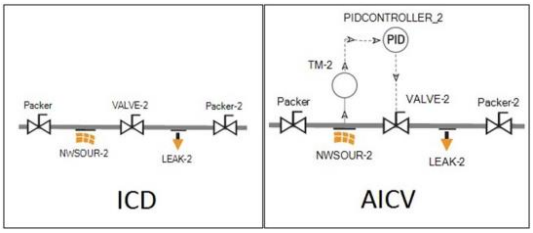

Figure 8. Set-up for one pipe section in OLGA.

There are no options to choose an autonomous inflow control valve in OLGA. The function of an AICV is therefore modeled using a transmitter and a PID regulator. The PID regulator was given a set-point of water cut (WC), and the valve opening was based on the actual WC. Figure 9 shows the outlet of the production pipe (Flowpath) with a choke and a PID regulator, which regulates with regards to the total flow rate. This system is implemented to account for the maximum capacity of an oil refinery and has a set point at 100 m^3/h.

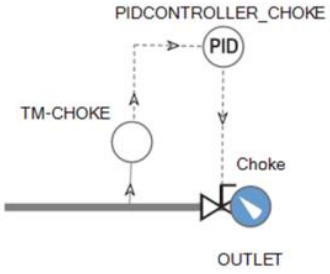

Figure 9. Sketch of the well outlet including a choke with a PID regulator.

3.1.4 Oil production with CO_2 EOR

Case 3, enhanced oil recovery using CO_2 in combination with AICV, is prepared for simulations. Case 3 was simulated with CO_2 already injected in the water phase. To avoid CO_2 short-circuiting between injectors and producers, AICVs were installed along the pipeline. AICVs close off the zones with early breakthrough of CO_2 and water, and ensure that CO_2 will be evenly distributed in the reservoir. The initial oil saturation in the reservoir for Case 1 and 2 is 100%, whereas the oil saturation for Case 3 is 50%.

The relative permeability changes when CO_2 is injected to a reservoir, and the oil is getting more mobile due to oil swelling, reduced viscosity and decrease of the interfacial tension. The relative permeability curves are adjusted and implemented in Rocx. Figure 10 shows the relative permeability curves for oil and water with and without CO_2.

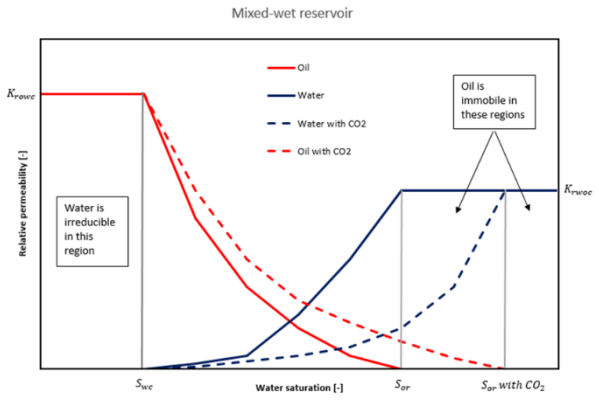

Figure 10. Relative permeability curves for oil and water; with and without CO_2 injection.

The residual oil saturation is reduced from 0.3 to 0.1 when CO_2 is injected to the reservoir. The irreversible water saturation is set to 0.2 in all the cases.

3.2 CO_2 storage

Before injecting supercritical CO_2 ($scCO_2$) into a reservoir or an aquifer, the storage capacity has to be evaluated. The storage capacity can be calculated based

on the model developed by Szulczewski and Juanes (Szulczewski and Juanes, 2009):

$$C_s = \left[\frac{2M\Gamma^2(1-S_{wc})}{\Gamma^2+(2-\Gamma)(1-M+M\Gamma)}\right]\rho_{scCO_2}\phi HWL_{total} \quad (6)$$

where C_s is the storage capacity, M is the mobility ratio, Γ is the trapping coefficient, S_{wc} is the connate water saturation, ρ_{scCO_2} is the density for $scCO_2$, ϕ is the porosity, H is the thickness of the sandstone, W is the length of the injection array, and L_{total} is the total length of the simulated reservoir. The bracketed term in Equation (6) is the storage efficiency and relates the total pore volume to the volume of trapped CO_2. The mobility ratio is defined as:

$$M = \frac{1/\mu_w}{K^*_{rCO_2}/\mu_{CO_2}} \quad (7)$$

where μ_w is the viscosity of brine, μ_{CO_2} is the viscosity of $scCO_2$, and $K^*_{rCO_2}$ is the endpoint relative permeability to $scCO_2$. The viscosities used for brine and $scCO_2$ are 0.5 and 0.043 cP, respectively. The trapping coefficient is defined as:

$$\Gamma = \frac{S_{rCO_2}}{1-S_{wc}} \quad (8)$$

where S_{rCO_2} is the residual saturation of CO_2. The Szulczewski and Juanes model also includes an equation for the CO_2 footprint, which is used to calculate how far the CO_2 plume migrates away from the injection array when it is completely trapped.

$$L_{max} = \left[\frac{(2-\Gamma)(1-M(1-\Gamma))}{(2-\Gamma)(1-M(1-\Gamma))+\Gamma^2}\right]L_{total} \quad (9)$$

Figure 11 illustrates the CO_2 footprint.

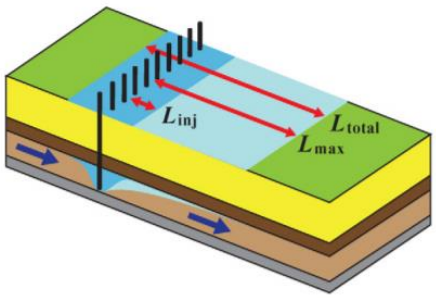

Figure 11. Injection and trapped CO_2 footprint (Szulczewski and Juanes, 2009)

The dark blue footprint is injection footprint and is measured as L_{inj}, the light blue footprint is the trapped footprint and is measured as L_{max}. The total plume after it is trapped is L_{total}.

As this is a simple model, it includes several assumptions. The reservoir is assumed to be horizontal, homogenous and isotropic, and the injected plume migrates with the aquifer flow. The fluid properties, such as viscosity and density, are assumed to be constant. (Szulczewski and Juanes, 2009)

4 Results

4.1 Oil production with ICD and AICV

A simulation model is developed based on the available information from the Johan Sverdrup field in the North Sea. The oil is classified as light oil, because of its high mobility with rather low viscosity and density. Two initial cases were simulated, one with ICDs and one with AICVs. The reservoir has an underlying aquifer, and the AICVs are used to close for water from this aquifer. Figure 12 presents the accumulated water production from the two cases. After about 200 days of production, the set point for the water cut is reached, and the AICVs start to close, to reduce the water production. The ICDs are passive devices, and do not have the ability to close for water. After 600 days, the accumulated water is 2.6 times higher for Case 1 compared to Case 2.

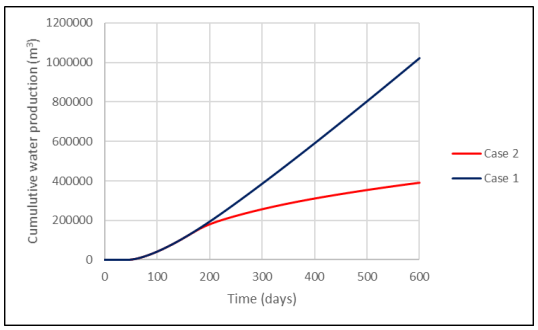

Figure 12. Water production versus time for Case 1 and Case 2.

The oil production from the two cases is compared in Figure 13. During the first 200 days, the oil and water production is equal for Case 1 and Case 2. This is because the AICVs in fully open position have the same inflow area as the ICDs. However, after the initial 200 days, when the AICVs have started to close, the oil production in Case 1 is higher than in Case 2. After 600 days of production, the accumulated oil for Case 1 is about 10% higher than for Case 2.

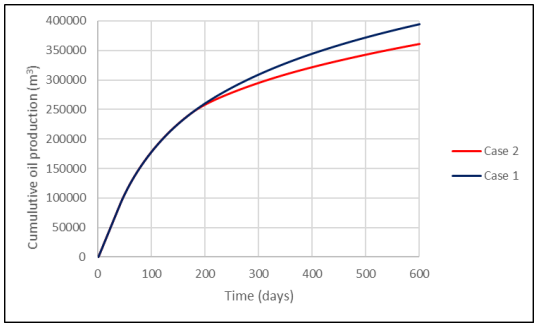

Figure 13. Oil production versus time for Case 1 and Case 2.

4.2 Enhanced oil recovery by injecting CO_2

Case 3, with CO_2 injection, can be considered as a continuation of Case 2. The initial oil saturation is determined to be 50%, which is the average oil saturation in Case 2 after 600 days. The simulation is performed assuming that CO_2 is already injected and well distributed in the reservoir. As the simulation with CO_2 was initiated with higher water saturation and lower oil saturation, it is expected that the flow control valves would begin throttling down sooner than the case with higher initial oil saturations. From Figure 14, it is can be seen how the AICVs close with time. The closure of the AICVs is determined by the water cut, and after about 300-400 days, it seems like all the AICVs are closed. In closed position, the AICVs, in this case, are producing from about 5% of the fully open valve area. After 600 days, the oil production can still be maintained as long as it provides a financial gain. After 600 days, the accumulated oil and water production is about 92000 m^3 and 189000m^3 respectively, and the average water cut is about 67%.

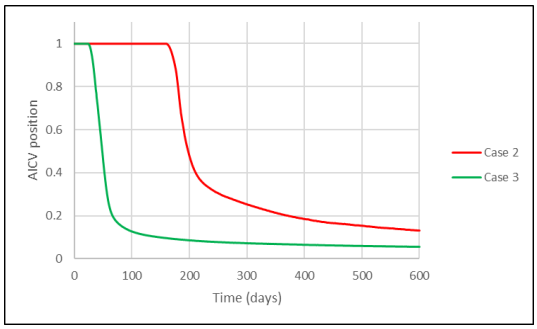

Figure 14. AICV position versus time.

4.3 Comparison of the results

Petroleum companies want a high oil/water ratio for their production chain. Water produced together with the oil results in problems for the oil industry, both economically and environmentally. The water cannot be pumped directly back to the sea, but requires cleaning to comply with national and international environmental policies. Thus, an effort to reduce water production but keep the oil production as high as possible is crucial. Autonomous inflow control devices, such as AICV, are developed to meet this challenge. Figure 15 shows a typical oil production case with ICD (Case 1), and an improved oil production case with the implementation of AICV (Case 2). Wells with ICD completion delay the water breakthrough in the same way as AICV completed wells, but as soon as the breakthrough occurs, the ICDs are not capable of choking the flow, and significant amounts of water are produced together with the oil. After water breakthrough, the AICVs are closed one by one. In a homogeneous reservoir, the drawdown, and thereby the production rate is highest in the heel section, and the earliest water breakthrough will occur in this section. When zones with water breakthrough are closed off, oil can still be produced from the other zones. Therefore, the AICV case are producing almost the same quantity of oil as the ICD case, but significantly less water.

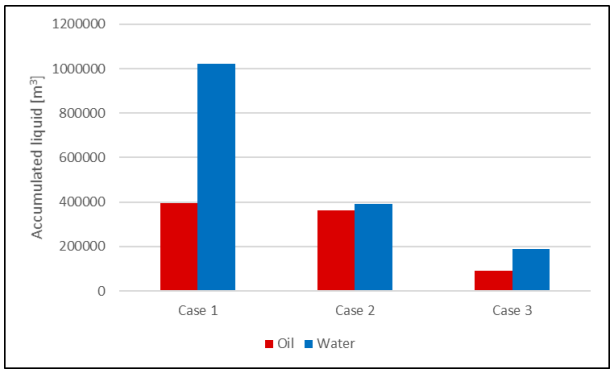

Figure 15. Comparison of accumulated oil and water.

The figure also shows the water and oil produced from the CO_2 injection case (Case 3). CO_2 EOR is mainly used in mature oil fields to increase the oil recovery. Case 3 is therefore run with an oil saturation of 50%. CO_2-injection changes the oil properties, and makes the oil more mobile. It is therefore possible to increase the oil recovery. When CO_2 injection is combined with AICV completion, the oil recovery can be increased without producing large amounts of water. CO_2-EOR is used to extract more oil from the reservoir when normal production is finished. The oil/water ratios for Case 1, Case 2 and Case 3 are 0.39, 0.92 and 0.49 respectively.

4.4 CO_2 storage capacity, Johan Sverdrup

The storage capacity model is used to give an intuitive picture of how much CO_2 can be stored in the Johan Sverdrup field. The area of the Johan Sverdrup field is about 200 km, and the reservoir thickness is set to 40 m. This gives a total volume of $8 \cdot 10^9$ m^3. The storage capacity and the CO_2 plume together with the properties of supercritical CO_2 are presented in Table 2. The storage capacity for CO_2 in the Johan Sverdrup field is found to be 49 megaton.

Table 2. CO_2 storage capacity and plume dimensions.

Parameter	**Value**
ϕ	0.28
S_{wc}	0.3
S_{rCO2}	0.4
k^*_{rCO2}	0.6
μ_{scCO_2}	0.000043 Pa·s
ρ_{scCO_2}	562 kg/m^3
Results	
C_s	$4.9 \cdot 10^7$ ton
L_{max}	≈20 km
$L_{injection}$	≈5 km
Efficiency factor	3.9%

Figure 16 presents the distribution of CO_2 in the reservoir and underlying aquifer. The red dot visualize the injection points, the light blue footprints is the trapped footprint, and the dark blue footprints is the injection footprint. It is assumed that the injected CO_2 migrates north of the injection point.

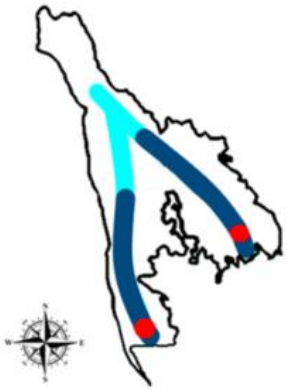

Figure 16. Hydrogeological footprint of CO_2 at Johan Sverdrup.

The information on the aquifer in the Johan Sverdrup reservoir is scarce. The visualized migration of the CO_2 plume from the injection point is therefore a hypothetical scenario, where the CO_2 follows the aquifer flow. The assumption made is that the plume migrates to the north of the injection point.

5 Conclusion

The objective of this paper is to study the CO_2 injection at the Johan Sverdrup field. The study included near-well simulations of oil production and CO_2 injection using the simulation tool OLGA in combination with Rocx. Three different cases were simulated for an intermediate-wet reservoir with high permeability, low oil viscosity, and low oil density. Production with inflow control devices (ICD) and autonomous inflow control valves (AICV) shows that AICVs have an average oil-to-water ratio of 0.92 compared to 0.39 for ICDs. CO_2-EOR in combination with AICVs, shows improved oil recovery, low water production, and low CO_2 reproduction. CO_2 injection into the Johan Sverdrup field increases oil recovery by approximately 33%. Oil produced from Case 1 (ICD), Case 2 (AICV), and Case 3 (CO_2 and AICV) is 395 000 m^3, 361 000 m^3, and 92 000 m^3, respectively. CO_2 EOR and storage are heavily dependent on the petrophysical properties of the reservoir. The CO_2 storage capacity for the Johan Sverdrup field is calculated to be 49 megatons, with an efficiency factor of 3.9%. The storage capacity is considered as very promising for the Johan Sverdrup reservoir.

References

H. Aakre, The Impact of Autonomous Inflow Control Valve on Increased Oil Production and Recovery, Doctoral thesis, University of South-Eastern Norway (USN), Porsgrunn, 2017.

H. Aakre, B. Halvorsen, B. Werswick, and V. Mathiesen, Smart well with autonomous inflow control valve technology, *SPE 164348-MS, SPE Middel East Oil and Gas Show and Exhibition*, Barhain, March 2013.

H. Aakre, V. Mathisen, and B. Moldestad, Performance of CO2 flooding in a heterogeneous oil reservoir using autonomous inflow control. *Journal of Petroleum Science and Engineering*, 167: 654-663, 2018.

V. M. Birchenko, K. M. Muradov, and D. R. Davies, Reduction of the horizontal well's heel–toe effect with inflow control devices, *Journal of Petroleum Science and Engineering*: 244-250, 2010.

Equinor ASA, Facts about the Johan Sverdrup field, https://www.equinor.com/en/what-we-do/johan-sverdrup/johan-sverdrup-facts.html

Halliburton, "Inflow Control Devices: Extending the Life of Mature Field Wells," 30th May 2012. https://halliburtonblog.com/inflow-control-devices-extending-the-life-of-mature-field-wells/

R. Kais, V. Mathiesen, H. Aakre, G. Woiceshyn, A. Elarabi, R. Hernandez, First Autonomous Inflow Control Valve (AICV) Well Completion Deployed in a Field under an EOR (Water & CO2 Injection) Scheme, *SPE-181552-MS*, 2016.

Norwegian Petroleum Directorate, Resource report 2019, https://www.npd.no/globalassets/1-npd/publikasjoner/ressursrapport-2019/resource-report-2019.pdf.

Schlumberger Software ltd., OLGA/ROCX, https://www.software.slb.com/products/olga/olga-wells-management/rocx [Accessed 11th March 2020]

S. M. Sund, T. B. Iversen, M. S. Hansen, J. Bohlin, O. K. Vøllestad, N. C. I. Furuvik, B. M. Halvorsen, Simulation of Oil Production from Homogenous North Sea Reservoirs with Inflow Control using OLGA/Rocx, *Linköping Electronic Conference Proceedings*, 138: 188-195, 2017.

M. Szulczewski and R. Juanes, A simple but rigorous model for calculating CO2 storage capacity, *Energy Procedia*, 1, 2009.